

Electroexcitation of odd-parity states in ^{27}Al

R. S. Hicks, A. Hotta,* J. B. Flanz,[†] and H. deVries[‡]

University of Massachusetts, Amherst, Massachusetts 01003

(Received 13 September 1979)

Inelastic electron scattering form factors were measured for the low-lying odd-parity states of ^{27}Al over a momentum transfer range of 0.57 to 2.41 fm^{-1} . Reduced ground-state transition probabilities were deduced for states at 4.055 MeV($1/2^-$), 5.156 MeV($3/2^-$), 6.159 MeV($3/2^-$), 6.477 MeV($7/2^-$), 6.605 MeV($1/2^-$ or $3/2^-$), 6.651 MeV($5/2^-$), 6.993 MeV($3/2^-$), and 7.228 MeV($9/2^-$). In addition, the results support odd-parity assignments for the 5.827 MeV($3/2^-$ or $5/2^+$) and 7.477 MeV($7/2^-$) levels. Attempts have been made to interpret the results in terms of the weak-coupling and strong-coupling models. The measurements confirm the apparent high concentration of $1p$ -shell proton hole strength in the 4.055 MeV, $1/2^-$ and 5.156 MeV, $3/2^-$ states. To satisfactorily account for the observed properties of these two levels using the weak-coupling model requires an anomalously small value of 1.35 MeV for the spin-orbit splitting of the $1p$ shell. The structure of levels in the 6 to 7.5 MeV region is shown to be based on the excitation of $1d$ -shell nucleons into the $1f$ shell.

NUCLEAR REACTIONS $^{27}\text{Al}(e, e')$, $E=70\text{--}340$ MeV; measured $\sigma(E; \theta)$, DWBA analysis. $\pi=-1$ levels, deduced $B(\lambda)$, δ . Strong-coupling model, weak-coupling model.

I. INTRODUCTION

In contrast to the even-parity states, the low-lying odd-parity states of the $2s\text{--}1d$ shell nuclei have received relatively little attention, either experimental or theoretical. For example, whereas reasonably successful shell-model calculations of the even-parity spectra can be made by considering only the sd -shell configuration space,¹⁻³ any realistic calculation of the negative-parity levels would have to include active $1p$ and $2p\text{--}1f$ shells. In the absence of such theoretical work, approaches to the understanding of the structure of odd-parity states are usually based upon more collective descriptions.

The $2s\text{--}1d$ shell nucleus considered here, ^{27}Al , is frequently regarded as transitional in shape, intermediate between lower- Z , prolate rotational nuclei (^{25}Mg , ^{25}Al , and ^{26}Mg), and heavier nuclei of oblate deformation (^{28}Si and ^{29}Si). Nevertheless, available experimental evidence seems to suggest a clearly prolate character for ^{27}Al : The sign of the observed ground-state quadrupole moment is positive ($+0.140eb$),⁴ and a Nilsson-model interpretation⁵ of the low-lying level scheme favors a prolate deformation corresponding to $\eta=3$. On the other hand, a simple rotational description of ^{27}Al is not nearly as convincing as it is for the $A=21\text{--}25$ nuclei. More satisfactory interpretations invoke appreciable band mixing,⁶ the coupling of rotational and vibrational motions,⁷ the strong interaction of particles in different Nilsson-model orbits,⁸ or the weak coupling of a proton hole to the collective rotational levels of a ^{28}Si core.⁹⁻¹³ Even

so, insofar as the even-parity states are concerned, none of these models is as comprehensively successful as the shell model calculations of Cole *et al.*² or Wildenthal and McGrory.¹

Recent (p, γ) measurements by Maas and collaborators¹⁴ have done much to clarify the spin-parity assignments of low-lying levels in ^{27}Al . The odd-parity spectrum shown in Fig. 1 is principally based upon two different configurations, one represented by the excitation of an sd -shell nucleon into the pf shell, and the other by the creation of a $1p$ -shell proton hole in the ground state of ^{28}Si . A comparison of data from pickup and stripping reactions¹⁵ indicates that the 4.055 MeV, $J^\pi = \frac{1}{2}^-$ and the 5.156 MeV, $\frac{3}{2}^-$ levels are hole states, and that the 6.159 MeV, $\frac{3}{2}^-$ and 6.477 MeV, $\frac{7}{2}^-$ states arise from particle excitation into the pf shell. In the framework of the Nilsson¹⁶ model, Ropke *et al.* identified the latter pair of states as the lowest two members of the $K^\pi = \frac{1}{2}^-$, $[330]$ rotational band.¹⁵ This identification is supported by observed similarities with negative-parity states in neighboring nuclei.

Presented in this paper are electron scattering form factors for most of the odd-parity states identified in ^{27}Al up to an excitation energy of 7.5 MeV. The availability of these form factors permits further tests to be made of the various models proposed for the structure of this nucleus. Previous electron scattering experiments^{6, 9, 17, 18} have not defined the form factors of the odd-parity spectrum, primarily because these experiments lacked the resolution to cope with the increasing level density at excitations in excess of 4 MeV.

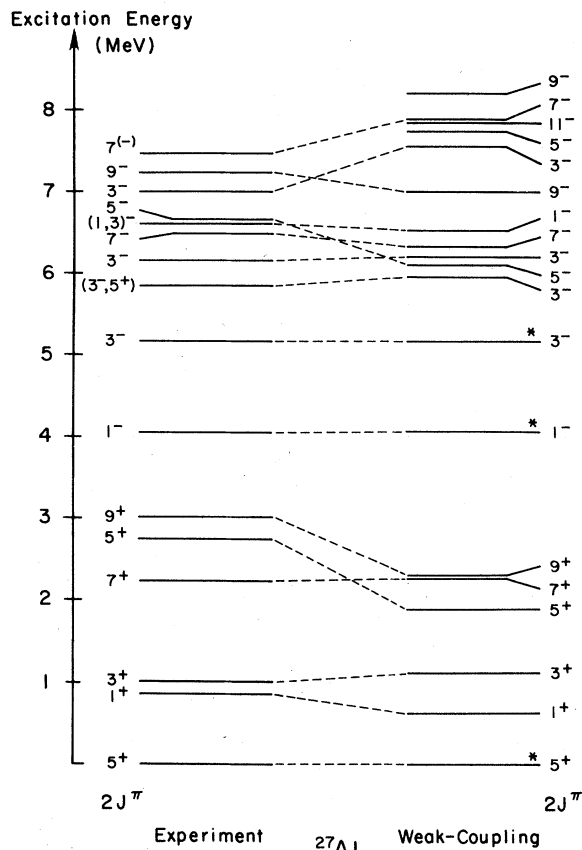


FIG. 1. Experimental and weak-coupling level schemes for ^{27}Al . Only the lowest-lying even-parity states are shown. An asterisk denotes that the corresponding weak-coupling level was fitted exactly to the energy of an observed state.

II. EXPERIMENTAL DETAILS

The measurements were performed using the 22-section linear accelerator of the Bates Laboratory in Middleton, Massachusetts. This S-band device can accelerate electrons to energies of 350 MeV or more with a duty factor of about 0.5%. The energy-analyzed beam emerges from the beam switchyard with a horizontal momentum dispersion which is rotated to the vertical plane by a system of five quadrupole lenses. When the beam is subsequently intercepted by the target it has a momentum dispersion of 10 cm/% and usual beam-spot dimensions of approximately 1 mm wide by 30 mm high.

For the experiment reported here, average on-target beam currents of up to 55 μA were delivered within a momentum spread of $\pm 0.15\%$. Beam currents were monitored by means of two identical ferrite toroids,¹⁹ the calibration of which had been previously established using the Faraday cup at the National Bureau of Standards Laboratories in

Maryland. Further details of the Bates electron accelerator and beam-handling system are given in Refs. 20 and 21.

Scattered electrons were momentum analyzed in a 900 MeV/c, split-pole magnetic spectrometer²² having a 2.23 m mean bending radius and a total deflection angle of 90° . The maximum spectrometer aperture subtended at the target was 26.8×130.9 mrad, corresponding to an acceptance solid angle of 3.514 msr.

The spectrometer focal plane instrumentation²³ consists of a pair of multiwire drift chambers and two Čerenkov counters. The Čerenkov counters fulfil three separate functions: They assist in the rejection of stray room background, provide information for the assessment of counting losses due to the wire-chamber dead time, and supply the timing start pulse for the delay-line circuit which measures the trajectory of incoming electrons. In the first wire chamber, the positions of the electrons in the momentum-dispersion direction are determined with a spatial resolution of 0.12 mm. Further trajectory information, from both chambers, is used to correct for focal-plane curvature and other spectrometer aberrations.²³ In the course of the present experiment, momentum resolutions as fine as 26 keV were obtained operating in the dispersion-matching mode.²² The useful momentum bite spanned by the focal-plane detection system is approximately 5%.

Measurements were performed at three scattering angles: 90° , 160° , and 180° . The 180° data were collected as an adjunct to a separate experiment to determine the cross section for elastic magnetic scattering.²⁴ When 180° scattering is being measured, an additional four-magnet system is employed to deflect backscattered electrons into the spectrometer.²⁵ The targets used in this experiment were high-impurity aluminum foils of thickness 6.62 to 30.6 mg cm^{-2} .

III. ANALYSIS OF DATA

A preliminary step in the analysis procedure was to determine the spectrometer momentum calibration. In the momentum-dispersion direction of the focal plane, the position x of an electron, momentum k_2 , can be parametrized by²²

$$x = x_s + (x|\delta) \left(\frac{k_2 - k_s}{k_s} \right) + (x|\delta\delta) \left(\frac{k_2 - k_s}{k_s} \right)^2, \quad (1)$$

where $(x|\delta)$ and $(x|\delta\delta)$ are first and second order spectrometer dispersion coefficients, and x_s and $k_s = 66.85 B$ MeV/c correspond to the central trajectory for a spectrometer field of B kG. From the reaction kinematics,²⁶ an electron scattering from a level of excitation energy ω_i will have mo-

mentum

$$k_2 = \frac{k_1 - \omega_i - \frac{\omega_i^2}{2M}}{1 + \frac{2k_1}{M} \sin^2 \frac{\theta}{2}} - \epsilon, \quad (2)$$

where k_1 is the incoming electron momentum, θ the scattering angle, M the mass of the target nucleus, and ϵ is the ionization energy loss.

By observing the focal-plane positions of several well-known peaks in the spectra of electrons scattered from targets of at least two different masses, the values of the unknowns, $(x|\delta)$, $(x|\delta\delta)$, x_s , and k_1 , can be accurately determined.

Corrections were applied for wire-chamber counting losses and the raw data were bin sorted. No corrections were applied for variation in the relative detection efficiency along the length of the chamber, since measurements have repeatedly shown the response to be flat, within a percent or so, across a broad range.²⁷ A representative bin-sorted spectrum is shown in Fig. 2.

Notwithstanding the fine momentum resolution of this experiment, the density of states at higher excitation energies necessitated the use of a line-shape fitting procedure to extract the integrated counts for each peak. The excitation spectra were divided up into convenient 1–3 MeV regions, each of which was individually fitted by an empirical polynomial background and a set of resonant peak functions $\phi_i(\omega, \omega_i)$ centered at various excitation energies ω_i :

$$\begin{aligned} \text{Counts}/(\text{Coulomb MeV}) = & A + B\omega^{\pm 1} + C\omega^{\pm 2} \\ & + \sum_i a_i \phi_i(\omega, \omega_i). \end{aligned} \quad (3)$$

The background coefficients A , B , and C are free

parameters, determined in the fit.

The line-shape function $\phi_i(\omega, \omega_i)$ is defined by several different processes which take place in the measured target. Most important of these are the emission of soft and virtual photons during scattering, hard-photon bremsstrahlung, and radiation and ionization straggling. The observed line shape is obtained by convoluting the distributions for these processes, together with an empirical function which characterizes not only the strength distribution of the measured nuclear state, but also the response of the particular experimental system, which is dependent upon the finite spatial resolution of the detector system and upon optical uncertainties in the accelerator, beam-handling system, and spectrometer. A detailed examination of the total electron scattering line-shape function has been made by Bergstrom.²⁸

From our point of view, an important aspect of the line shape is that the dependence of the so-called "radiative tail"²⁸ be given accurately, especially in the region close to the associated spectrum peak. This importance stems from our method of computing the differential cross sections. The total number of counts in a particular peak is determined by integrating the fitted curve out towards the low-energy scattered electron side. The integration is continued until some specified cutoff energy Δ below the energy of the peak E_2 and corrections for the previously mentioned radiative and ionization processes are then applied. If the shape of the tail is appropriate, corrected areas obtained to various integration cutoffs should closely agree.

Insofar as the complete calculation of the line-shape function is rather time consuming, we have used an alternative, approximate method to gene-

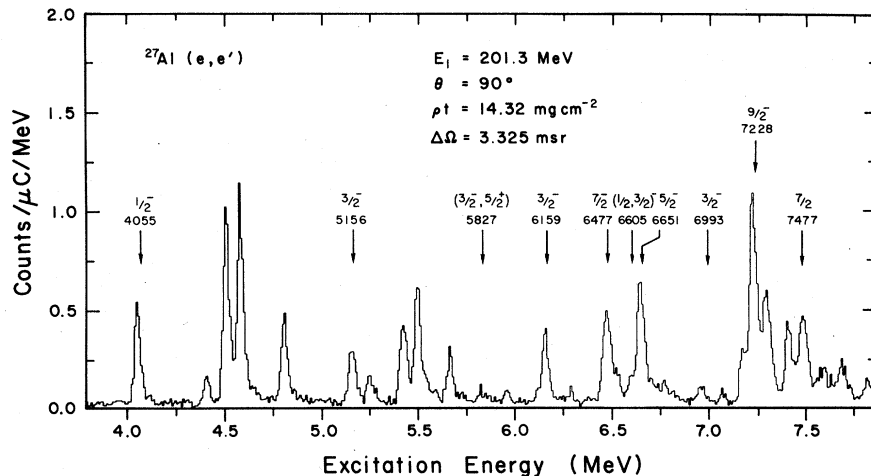


FIG. 2. Identification of ^{27}Al odd-parity states in a representative bin-sorted spectrum. A target of thickness 14.3 mg cm^{-2} was used in transmission geometry.

rate the line shape.²⁹ This derives from the functional form of the predominant Schwinger correction factor,²⁶

$$S(\Delta) = \exp[-\delta_s(\Delta)], \quad (4a)$$

where

$$\delta_s(\Delta) = \kappa \left[\ln \left(\frac{E_1^{1/2} E_2^{1/2}}{\Delta} \right) - \frac{13}{12} \right] + (2\alpha/\pi) \left\{ \frac{17}{36} + \frac{1}{4} \ln^2 \left(\frac{E_1}{E_2} \right) + \frac{1}{2} \left[\frac{\pi^2}{6} - L_2 \left(\cos^2 \frac{\theta}{2} \right) \right] \right\}, \quad (4b)$$

E_1 being the incident electron energy, and L_2 the Euler dilogarithm. The parameter κ , given by

$$\kappa = (2\alpha/\pi) [\ln(q^2/m_e^2) - 1], \quad (4c)$$

may be altered slightly to incorporate contributions from radiation and ionization straggling corrections. Given the dependence of Eq. (4b), it may then be shown that the proper line-shape function can be well approximated by²⁹

$$\phi(E) = \kappa \frac{\int_{E+d}^{\infty} \phi_0(E') dE'}{\int_{E+d}^{\infty} (E' - E) \phi_0(E') dE'} \times \int_{E+d}^{\infty} \phi(E') dE' + \phi_0 \left(E + \frac{d}{2} \right) S(d), \quad (5)$$

where d is the bin-sort channel width and ϕ_0 describes the peak shape in the absence of radiation and ionization effects. Proceeding from the high-energy scattered electron side, the line-shape function for a particular peak may then be calcu-

lated.

The choice of the function ϕ_0 is somewhat arbitrary. We have used asymmetric Gaussian parametrizations, Lorentzians, and Fermi-type functions for cases of relatively thick targets in reflection geometry. In any case, the particular form of ϕ_0 is important only within approximately 2 full width at half maximum (FWHM) of the peak position. At lower scattered electron energies, the shape of the radiative tail is strongly determined by calculable parameters entering into the equations for the radiation correction factors. It has been found that this method of calculating the line-shape function is quite amenable to interactive analysis carried out on small computers, such as the PDP 11/40 used in the present case.

An example of a line-shape fitted spectrum is shown in Fig. 3. The absolute scale of the deduced differential cross sections was established by normalizing a set of ^{12}C elastic scattering measurements, taken concurrently during the course of the Al experiment, to the ^{12}C cross section of Sick and McCarthy.³⁰ At 180° , where scattering from the spinless ^{12}C nucleus is much reduced, the data were normalized to the proton cross sections.³¹

A more explicit and convenient comparison with theory can be obtained by transforming the measured cross sections into electron scattering form factors³²:

$$\sigma(E, \theta) = \frac{2Z^2\alpha^2}{q_\mu^4} \frac{k_2}{k_1} \frac{V_L}{1 + (2k_1/M) \sin^2\theta/2} |F(k_1, \theta)|^2, \quad (6)$$

where k_1 and k_2 are the initial and final electron momenta and q_μ is the four-momentum transfer,

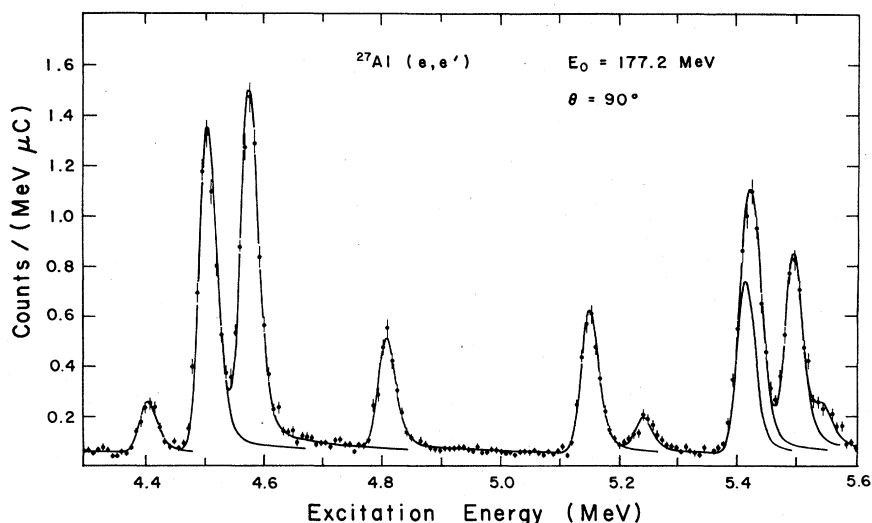


FIG. 3. Example of line-shape fitting analysis. The peak positions are fixed to tabulated excitation energies, and all peak widths are assumed equal.

given to good approximation by

$$q_\mu^2 = 4k_1k_2 \sin^2\theta/2. \quad (7)$$

In the plane-wave Born approximation, the form factor separates into longitudinal and transverse components, dependent only upon the three-momentum transfer q :

$$|F(q)|^2 = |F_L(q)|^2 + \frac{V_T}{V_L} |F_T(q)|^2, \quad (8)$$

$$q^2 = (\vec{k}_1 - \vec{k}_2)^2. \quad (9)$$

For our purposes, the coefficients V_L and V_T are given sufficiently well by

$$V_L = \frac{1}{2} \frac{q_\mu^4}{q^4} \left[4k_1k_2 \cos^2\theta/2 + m_e^2 \left(2 + \frac{k_1}{k_2} + \frac{k_2}{k_1} \right) \right] \quad (10a)$$

and

$$V_T = \frac{1}{2} \frac{q_\mu^2}{q^2} [(k_1+k_2)^2 - 2k_1k_2 \cos^2\theta/2], \quad (10b)$$

where m_e is the electron rest mass.

For the present data, obtained using many different incident electron energies, comparison with theoretical models would normally be a tedious procedure in that each different energy requires a separate distorted-wave calculation. However, tests showed that it was adequate to compare the data with a single distorted-wave result calculated for one incident energy (250 MeV), provided that both the data and the calculated curve are plotted against an "effective" momentum transfer,³³ given by

$$q_{\text{eff}} = q \left(1 + \frac{3Z\alpha}{2k_1R} \right). \quad (11)$$

The parameter R represents the "uniform-density" charge radius, 3.94 fm for ^{27}Al .

In the course of the experiment inelastic form factors were obtained for both odd- and even-parity levels up to 8 MeV excitation energy. Of the levels tabulated by Endt and van der Leun,⁴ only the 5.752 MeV, $\frac{1}{2}^+$ state remained unobserved below 6 MeV. In the entire measured spectrum, the only established odd-parity state not to be observed was the $\frac{3}{2}^-$ state at 6.993 MeV. The data span a momentum transfer range of 0.57 to 2.41 fm^{-1} , with low- q measurements being sparse for the higher excited states. Although the focus of this paper is constrained to the odd-parity spectrum, a large quantity of data was also collected on even-parity levels. This will be presented at a later date.³⁴ Complete tables of cross sections and form factors are available from the authors.

IV. RESULTS

Theoretical C3 form factors for the most likely single-particle transitions are shown in Fig. 4.

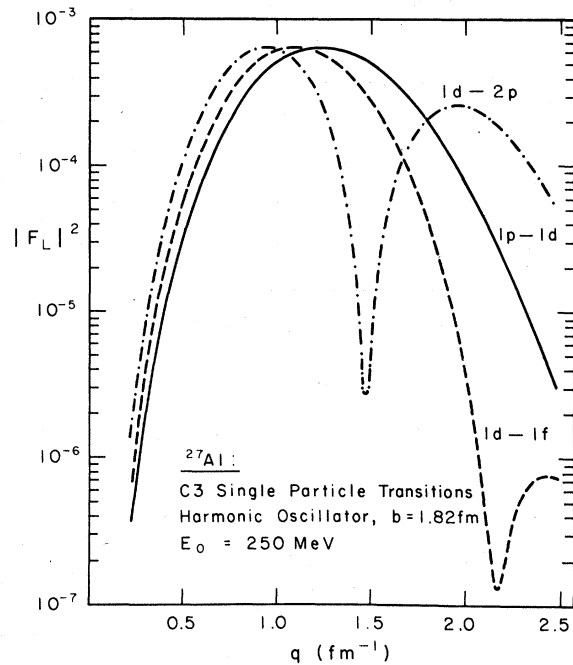


FIG. 4. Comparison of C3(e, e') form factors for single-particle, odd-parity transitions in ^{27}Al . The form factors were computed in the distorted-wave Born approximation using harmonic oscillator radial wave functions with a range parameter b equal to 1.82 fm. The magnitudes of the form factors have been arbitrarily normalized to emphasize the different q dependences.

These have been computed in the harmonic oscillator model, with a value of 1.82 fm for the oscillator size parameter b . Although a small degree of freedom is commonly permitted in this parameter, meaningful theoretical interpretations require it to lie within 5–10% of the value determined from the ground-state rms charge radius. For ^{27}Al this value is 1.815 ± 0.030 fm.^{35,36}

In view of the recognized collective nature of the ^{27}Al inelastic spectrum, we might not expect to observe the pure transition q dependences shown in Fig. 4; at least some degree of configuration mixing is anticipated. Nonetheless, a comparison of these calculations with the observed form factors should permit identification of the essential underlying character of the various odd-parity states. A detailed examination of the various measured form factors now follows.

The measured longitudinal form factors were predominantly of C3 character. Except for the form factor of the 5.156 MeV, $\frac{3}{2}^-$ state, evidence for C1 strength was minimal. Form factors deduced for the 4.055, 5.156, and 5.827 states are shown in Fig. 5. The observed momentum transfer dependence identifies these levels as proton-hole states, rather than states involving the pro-

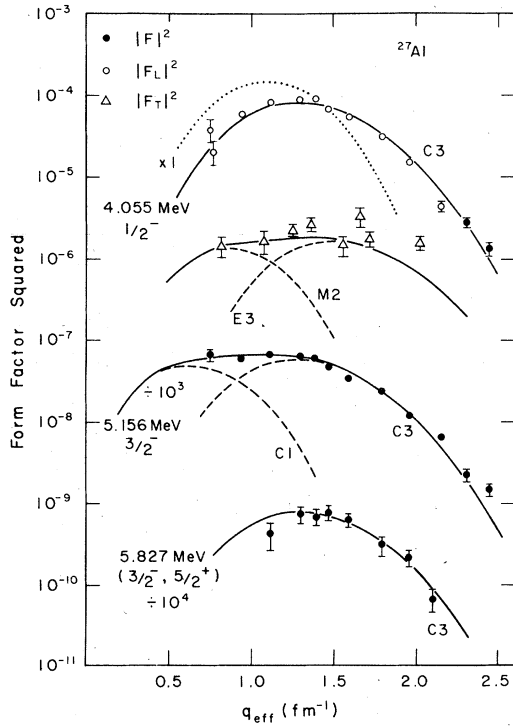


FIG. 5. Inelastic form factors measured for $1p$ -hole states in ^{27}Al , and comparison with best-fit theoretical curves. The calculated longitudinal form factors were obtained in the distorted-wave Born approximation using the single-particle, harmonic oscillator model with $b = 1.85$ fm. The q dependence of the data differs markedly from that expected for the $C3$ multipole of a $1d \rightarrow 1f$ transition, which is represented by a dotted curve at the top of the figure.

motion of a $d_{5/2}$ nucleon into the pf shell. This is in accord with the structure indicated by particle transfer reactions.¹⁵ The enhancement of the 5.156 MeV longitudinal form factor at low q discloses the existence of a measurable $C1$ component. No such

enhancement is observed in the form factor of the 4.055 MeV level. The experimental form factors are therefore consistent with the respective assignments of $\frac{3}{2}^-$ and $\frac{1}{2}^-$ made recently by Maas *et al.*¹⁴ The spin and parity of the 5.827 MeV level are currently restricted to two possibilities: $\frac{3}{2}^-$ or $\frac{5}{2}^+$. Our results for this state, although of relatively poor statistical precision, lend support to the odd-parity assignment.

The value of the harmonic oscillator parameter which best describes the momentum transfer dependence of the $1p$ -hole form factors is 1.85 ± 0.09 fm. The deduced $C1$ and $C3$ transition probabilities are listed in Table I. It is noted that the combined $C3$ strength of the 4.055 and 5.156 MeV states amounts to $(58 \pm 29)\%$ of the total single-particle strength allowed for excitation to $1p$ -shell proton-hole states.

By comparing the 90° data with the measurements made at backward scattering angles, we were able to determine the transverse form factor of the 4.055 MeV state. This form factor is also shown in Fig. 5. The shapes of the constituent $M2$ and $E3$ multipole components were again computed using the harmonic oscillator, single-particle model with $b = 1.85$ fm and the normalization of the $E3$ form factor was fixed to the $B(C3)$ value established previously, as required by Siegert's theorem. Adjusting the magnitude of the $M2$ component to give a best fit to the experimental form factor leads then to a deduced multipole mixing ratio for the decay to the ground state of

$$|\delta| = \left[\frac{\Gamma(E3)}{\Gamma(M2)} \right]^{1/2} = 0.11 \pm 0.03,$$

where the error includes a component corresponding to a $\pm 5\%$ variation in the parameter b .

Figure 6 shows 90° form factors deduced for odd-parity states in the 6 to 7.5 MeV region.

The q dependence of these form factors is charac-

TABLE I. Transition probabilities for excitations from ground state of ^{27}Al , deduced from harmonic oscillator model fits.

E_x^a (MeV)	$2J^\pi$	$B(C1^\dagger)$ ($e^2 \text{fm}^2$)	$B(C3^\dagger)$ ($e^2 \text{fm}^6$)	$B(C5^\dagger)$ ($e^2 \text{fm}^{10}$)	$B(M2^\dagger)$ ($e^2 \text{fm}^4$)
4.055	1^-		60 ± 25		0.034 ± 0.011
5.156	3^-	0.041 ± 0.011	41 ± 17		
5.827	$(3^-, 5^+)$		5.5 ± 2		
6.159	3^-		207 ± 44		
6.477	7^-		217 ± 32	$(8.0 \pm 3.0) \times 10^4$	
6.605	$(1, 3)^-$		86 ± 21		
6.651	5^-		367 ± 55	$(2.3 \pm 1.1) \times 10^4$	
6.993	3^-		<15		
7.228	9^-		604 ± 91	$(1.7 \pm 1.2) \times 10^4$	
7.477	7		281 ± 42	$(3.3 \pm 2.0) \times 10^4$	

^a Excitation energies and spin assignments taken from Ref. 4.

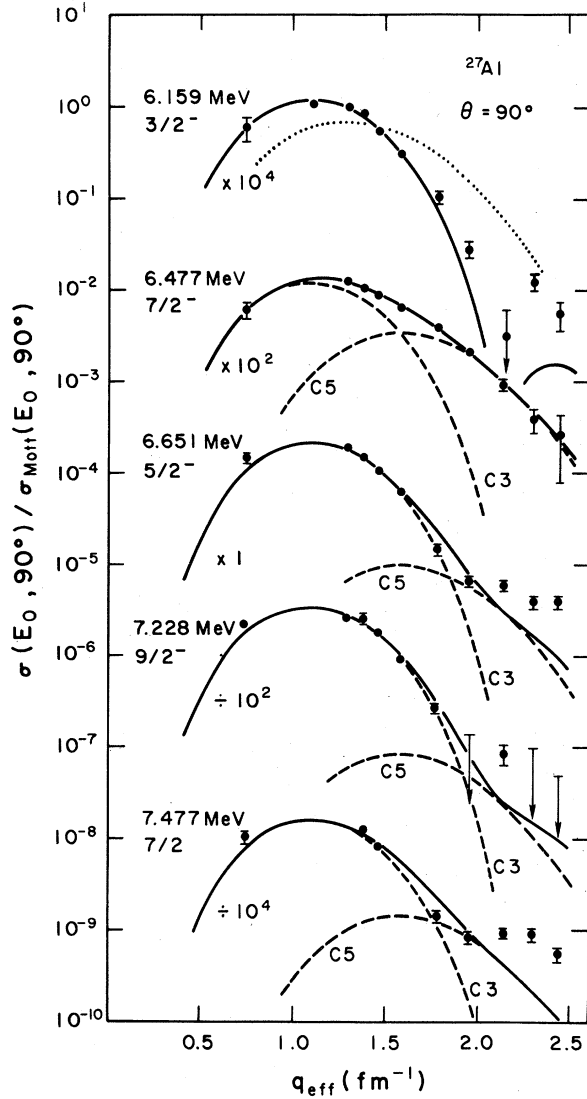


FIG. 6. Measured (e, e') form factors for ^{27}Al odd-parity states characterized, in large part, by the excitation of a $1d$ -shell nucleon into the $1f$ shell. For comparison, the q dependence expected for a $C3$ excitation to a $1p$ -hole state is shown by the dotted line at the top of the figure. The best-fit DWBA curves were calculated using the single-particle harmonic oscillator model with $b = 1.94$ fm. Transverse components were assumed to be small and are excluded from the calculated curves.

teristic of $1d-1f$ particle excitation, differing markedly from the dependence observed for the $1p$ -hole states. The best-fit value of the parameter b was 1.94 ± 0.05 fm, which represents a slight increase over the value obtained from the ground-state charge radius. This enhancement may reflect the presence of weak admixtures of other particle-hole configurations in the excited states, most probably configurations containing a

nucleon in the $2p$ -shell. Note, however, that in order to fit the observed form factors with the q dependences calculated for either the $1d-2p$ or $1p-1d$ transitions, respective b values close to 1.48 and 2.27 fm are required, values unacceptable for ^{27}Al . We conclude that the $C3$ excitation strength in the 6 to 7.5 MeV region originates mainly from $1d-1f$ particle transitions.

At a scattering angle of 90° , longitudinal strength is expected to dominate these form factors, except in the $q \geq 2$ fm $^{-1}$ region above the first maximum of the $C3$ multipole component, where the transverse contributions may be appreciable. The fitted $B(C5)$ values that are listed in Table I are therefore rather uncertain. In any case, only the $\frac{7}{2}^-$, 6.477 MeV level shows evidence of strong $C5$ excitation.

Three levels deserve individual mention. Two or three statistically imprecise data points, not shown in Fig. 6, were obtained on the $(\frac{1}{2}^-, \frac{3}{2}^-)$, 6.605 MeV level. Based on these points we were able to make a crude estimate for the strength of $C3$ excitation to this state. On the other hand, the failure to observe the $\frac{3}{2}^-$ state at 6.993 MeV meant that only an upper limit could be set for the $C3$ transition probability to this level. In order to do this, the form factor was assumed to have a q dependence similar to that of neighboring negative-parity states. Finally, although the parity of the $\frac{7}{2}^-$, 7.477 MeV state has yet to be identified, the close similarity of its form factor with those of established odd-parity states in the vicinity suggests that this state also belongs to the odd-parity spectrum.

V. STRONG-COUPLING MODEL

In the preceding section, the extreme single-particle model has been utilized to establish the underlying character of each observed odd-parity state. By following this procedure, we have been able to discriminate between the hole states and the particle states, and the conclusions reached are in accord with those indicated by data from pickup and stripping reactions. Moreover, by adjusting the single-particle parameters to fit the experimental form factors, reduced ground-state transition probabilities have also been deduced. It is clear, however, that the extreme single-particle model is unable to account for the large number of observed odd-parity states. The single-particle excitations are evidently coupled to more collective modes. In this section, and the one that follows, we therefore attempt to interpret the odd-parity states in terms of two collective models, the strong- and weak-coupling models.

The $\frac{3}{2}^-$ and $\frac{7}{2}^-$ levels at 6.159 and 6.477 MeV have been identified as the lowest two members of the

$K^\pi = \frac{1}{2}^-$, [330] rotational band which is based on the $1f_{7/2}$ subshell.¹⁵ It has long been recognized that strong decoupling inverts the ordering of this band, displacing the $J^\pi = \frac{3}{2}^-$ member to the position of lowest excitation energy.³⁷ This is followed by the $\frac{7}{2}^-$ and $\frac{1}{2}^-$ members. Although the odd-parity state at 6.605 MeV still bears an ambiguous spin assignment of $\frac{1}{2}^-$ or $\frac{3}{2}^-$, it is tempting to identify this as the $\frac{1}{2}^-$, third member of the [330] band, and to further assume that states at 6.651 and 7.228 MeV represent the $J^\pi = \frac{5}{2}^-$ and $\frac{9}{2}^-$ members. In the rotational model, the probable second $\frac{7}{2}^-$ state at 7.477 MeV and unobserved $\frac{3}{2}^-$, 6.993 MeV level must belong to a different band or bands.

The reduced transition probability for electromagnetic transitions of multipolarity λ between bands of angular momentum projections K and K' is given by¹⁶

$$B(E\lambda; JK \rightarrow J'K') = e^2 \left(\frac{\hbar}{M\omega_0} \right)^{2\lambda+1} \frac{2\lambda+1}{4\pi} G_{E\lambda}^2 \times |C(J\lambda J'; K K' - K K') + b_{E\lambda} (-1)^{J'+K'} \times C(J\lambda J'; K - K' - K - K')|^2, \quad (12)$$

where the second term contributes only for cases

in which $\lambda \geq K + K'$.

C3 transition rates computed using theoretical values¹⁶ of the coefficients $b_{E\lambda}$ and $G_{E\lambda}$ (which depend upon the nuclear deformation) unfortunately lie in poor agreement with the rates observed experimentally. In particular, the measured rates are not obtained unless the parameter G_{E3} is approximately doubled. We have therefore chosen to fit the values of b_{E3} and G_{E3} to the excitation strengths observed for two low-spin band members. The results presented in Table II correspond to

$$b_{E3} = -0.04$$

and

$$|G_{E3}| = 5.484.$$

With the solitary exception of the $\frac{9}{2}^-$ state, excellent agreement is obtained with the experimental $B(C3\uparrow)$ values. It is possible, of course, that the 7.228 MeV $\frac{9}{2}^-$ state in fact belongs to a different band. The true $\frac{9}{2}^-$ member of the [330] band is expected to be excited only weakly, and hence may have remained unobserved in this region of relatively high level density. The failure to locate a possible $\frac{1}{2}^-$ band member is scarcely surprising, in view of the very weak excitation strength pre-

TABLE II. Comparison of experimental excitation energies and transition probabilities with predictions of weak- and strong-coupling models.

$2J^\pi$	L	Experiment		Weak coupling		Strong coupling
		E_x^a (MeV)	$B(CL\uparrow)$ ($e^2 \text{fm}^{2L}$)	E_x (MeV)	$B(CL\uparrow)$ ($e^2 \text{fm}^{2L}$)	$B(CL\uparrow)$ ($e^2 \text{fm}^{2L}$)
1 ⁺	2	0.843	13.5 ± 1.0 ^b	0.62	37	
3 ⁺	2	1.013	27 ± 2 ^b	1.11	43	
7 ⁺	2	2.211	95 ± 10 ^b	2.27	65	
5 ⁺	2	2.734	8 ± 3 ^{b,d}	1.89	29	
9 ⁺	2	3.001	57 ± 3 ^b	2.30	129	
1 ⁻	3	4.055	60 ± 25	4.06 ^c	69	
3 ⁻	3	5.156	41 ± 17	5.16 ^c	39	
3 ⁻	3	5.827 ^e	5.5 ± 2	5.96	12.8	
5 ⁻	3			6.01	4.2	
1 ⁻	3	6.605 ^e	86 ± 21	6.52	74	55
3 ⁻	3	6.159	207 ± 44	6.20	156	207 ^c
3 ⁻	3	6.993	<15	7.55	95	251
5 ⁻	3	6.651	367 ± 55	6.09	398	367 ^c
5 ⁻	3			7.73	200	
7 ⁻	3	6.477	217 ± 32	6.32	898	232
7 ⁻	3	7.477 ^e	281 ± 42	7.87	151	1049
9 ⁻	3	7.228	604 ± 91	6.92	1282	90
9 ⁻	3			8.20	4	1286
11 ⁻	3			7.83	446	12
11 ⁻	3			9.12	405	

^a Reference 4.

^b References 4, 9, 34.

^c Parameter fitted specifically to measured value.

^d Assuming C0 excitation strength can be neglected.

^e Observed state has uncertain spin-parity assignment.

dicted for this state.

The existence of $K^\pi = \frac{1}{2}^-$ rotational bands based on 1p-hole states has long been recognized in the mass 21 and 23 nuclei. For example, band members up to $J^\pi = \frac{11}{2}^-$ have been identified in ^{21}Ne and ^{23}Na .³⁸ From the spectroscopic factors observed for proton pickup it is apparent, however, that the lowest-excited odd-parity states of ^{27}Al cannot similarly be interpreted as members of a single rotational band. The respective spectroscopic factors measured for the 4.055 MeV, $\frac{1}{2}^-$ and 5.516 MeV, $\frac{3}{2}^-$ states are 2.9 and 2.3,⁴ and since each Nilsson level can contain just two particles, the involvement of several different rotational bands is implied. That such bands may be strongly mixed is not unexpected, inasmuch as it is well known that the Coriolis interaction in sd -shell nuclei results in appreciable mixing of bands whose angular momentum projections K differ by $1\hbar$. (Such band mixing may also account for the necessity of having to increase the parameter $G_{\mathcal{E}_3}$ in order to generate the appropriate strength for excitation of members of the [330] band.³⁹) Furthermore, the sizable $C1$ multipole component in the form factor of the $\frac{3}{2}^-$, 5.516 MeV state also points to this level having a somewhat different structure from that of the $\frac{1}{2}^-$, 4.055 MeV state.

VI. WEAK-COUPLING MODEL

During the decades of the sixties and seventies, numerous attempts were made to describe the lowest-excited even-parity levels of ^{27}Al as resulting from the weak coupling of a $1d_{5/2}$ proton hole to the first excited 2^+ state of ^{28}Si (Refs. 9–13). Support for this interpretation came not only from the fact that the center of gravity of the relevant ^{27}Al levels lies close to the 1.779 MeV excitation energy of the ^{28}Si core state, as expected in the weak-coupling limit, but also from the measured inelastic scattering cross sections,^{12,13} which appeared to follow the predicted $(2J+1)$ strength rule. As both the range and precision of nuclear data have been progressively improved, several deficiencies have become apparent in the weak-coupling interpretation of these levels.⁹ For example, in the mid-sixties Thankappan¹⁰ and Evers *et al.*¹¹ independently obtained good fits to the observed energy levels and electromagnetic properties using the then unknown quadrupole moment of the ^{28}Si first 2^+ state as a free parameter. Their respective best-fit values of 0.035 and 0.017 eb were later shown to be in substantial disagreement with the experimentally observed moment, $+0.16 \pm 0.04$ eb (Ref. 40). Subsequent recalculations using the measured value experienced some difficulty in reproducing the observed properties of the

even-parity ^{27}Al levels, even when the weak-coupling basis was extended to include higher-excited ^{28}Si core states.⁹

Notwithstanding these problems, we elected to recompute the weak-coupling model once again, with particular emphasis on the negative-parity states. For the mid- sd -shell nuclei the weak-coupling model can be expected to provide a better description of the unnatural-parity $1\hbar\omega$ states than it does for states of $0\hbar\omega$ character. The lowest even-parity levels were retained in the calculation primarily for the sake of achieving reasonable self-consistency.

In the weak-coupling model, odd-parity states in the 6–8 MeV region of the ^{27}Al excitation spectrum can be constructed by coupling a $1d_{5/2}$ proton hole to the strongly collective 3^- state of ^{28}Si at 6.878 MeV. This representation is lent weight by the closely similar q dependences observed for the respective (e, e') form factors.^{41,42} However, as pointed out by Brain *et al.*⁴³ the 4^- core state at 8.413 MeV should also be included, since this is observed to be connected to the 3^- state by an appreciable $E2$ matrix element.

Following the formalism of Thankappan and True,⁴⁴ the core-hole interaction was assumed to consist of dipole and quadrupole terms:

$$H_{ch} = -\xi(J_c \cdot j_h) - \eta(Q_c \cdot Q_h), \quad (13)$$

where J_c and Q_c are the angular momentum and mass quadrupole operators for the core, and j_h and Q_h are the corresponding operators for the hole. The required core matrix elements were determined from measured electromagnetic transition rates and quadrupole moments or, where experimental data were lacking, were computed using the rigid rotor model.⁴⁵ $C2$ matrix elements for the $1d_{5/2}$ proton hole were calculated using harmonic oscillator radial wave functions with a size parameter of 1.815 fm. To perform the actual weak-coupling calculation, the program INTER⁴⁵ was used, with the strength parameters ξ and η being varied until a reasonable compromise solution was found for both the energy levels and the electromagnetic properties. The results summarized in Tables II and III correspond to the values $\xi = -0.113$ and $\eta = 0.00854$.

Before discussing these results, mention should be made of the basis chosen for the calculation of the lowest-lying odd-parity states at 4.055 and 5.516 MeV. These states were assumed to be given by the coupling of $1p_{3/2}$ and $1p_{1/2}$ proton holes to the 0^+ ground state and 2^+ first excited state of the ^{28}Si core nucleus. A similar construction has been used by Benson and Flowers⁴⁶ to compute the low-lying negative-parity spectrum of ^{19}F . Two additional parameters entering into the calculation

TABLE III. Weak-coupling eigenvalues and eigenvectors for low-lying states of ^{27}Al . Listed at the head of each column is the weak-coupling basis state, $|J_C J_h\rangle$.

E_x (MeV)	$2J$	$ 0^+ \frac{5}{2}\rangle$	$ 2^+ \frac{5}{2}\rangle$	$ 3^+ \frac{5}{2}\rangle$	$ 4^+ \frac{5}{2}\rangle$	$ 0^+ \frac{1}{2}\rangle$	$ 2^+ \frac{1}{2}\rangle$	$ 0^+ \frac{3}{2}\rangle$	$ 2^+ \frac{3}{2}\rangle$
0.00	5^+	0.9642	-0.2651						
0.62	1^+		1.0000						
1.11	3^+		1.0000						
1.89	5^+	-0.2651	-0.9642						
2.27	7^+		1.0000						
2.30	9^+		1.0000						
4.06	1^-					0.9823			0.1875
5.16	3^-						-0.5578	0.7934	-0.2438
5.96	3^-						-0.8065	-0.5875	-0.0666
6.01	5^-						0.9930		-0.1178
6.09	5^-			0.9292	0.3696				
6.20	3^-			0.9210	0.3897				
6.32	7^-			0.9686	0.2484				
6.52	1^-			1.0000					
6.92	9^-			0.9992	-0.0393				
7.55	3^-			0.3897	-0.9210				
7.73	5^-			0.3696	-0.9292				
7.83	11^-			0.8822	-0.4708				
7.87	7^-			0.2484	-0.9686				
8.20	9^-			-0.0393	-0.9992				
9.12	11^-			-0.4708	-0.8822				
9.78	13^-				1.0000				

of these states are $\epsilon_{p_{3/2}}$ and $\epsilon_{p_{1/2}}$, the energies of the $1p$ -shell proton holes relative to the $1d_{5/2}$ hole.

A comparison of the calculated and experimental⁴ level schemes is shown in Fig. 1. Only the lowest even-parity states are depicted. Given that the bulk of the theoretical spectrum is computed using only two free parameters, ξ and η , the level of agreement is generally quite fair. The calculations are seen to support the $\frac{3}{2}^-$ and $\frac{7}{2}^-$ assignments previously suggested for the states observed at 5.827 and 7.477 MeV.

The most notable deficiency of the model is the locating of the first excited $\frac{5}{2}^+$ state 0.85 MeV below the measured excitation energy. This has been a persistent problem in the weak-coupling interpretation of ^{27}Al .^{9,10} Moreover, as indicated in Table II, the predicted $B(C2^+)$ strength leading to this state exceeds the experimental value by a factor of approximately 3. With the exception of the 2.211 MeV $\frac{7}{2}^+$ state, the $B(C2^+)$ values for the even-parity states are also overestimated, although the calculated ground-state quadrupole moment of 0.136 eb lies in good agreement with the observed value, 0.140 ± 0.002 eb.⁴ Proton pickup measurements give rise to further misgivings in the weak-coupling description of the low-lying positive-parity spectrum. The pickup angular distribution for the $\frac{1}{2}^+$ 0.843 MeV state is characteristic of an $l=0$ angular momentum transfer, indicating that this level has a somewhat different

structure to that of the neighboring even-parity states, which are observed to have $l=2$ distributions.^{47,48}

Turning to the odd-parity states, measured $B(C3^+)$ values for the $\frac{1}{2}^-$, $\frac{3}{2}^-$, and $\frac{5}{2}^-$ levels in the 6–8 MeV excitation range are seen to be reasonably well described by the weak-coupling calculation. On the other hand, the strengths of the neighboring $\frac{7}{2}^-$ and $\frac{9}{2}^-$ states are substantially overestimated. To some extent this disagreement can be rectified by assuming greater mixing of the two sets of basis states; those formed by coupling to the 3^- 6.878 MeV state of the ^{28}Si core, and those constructed by coupling to the 4^- level at 8.413 MeV. However, the corresponding $E2$ matrix element appears to be reasonably well fixed by experiment,⁴⁹ and, in any case, any *ad hoc* increase in the magnitude of the matrix element leads to a rapid deterioration in the agreement between the observed and calculated energy level schemes.

The properties of the lowest-excited odd-parity states, those formed by coupling a $1p$ proton hole to the ^{28}Si core, prove to be rather sensitive to the values chosen for the proton-hole energies $\epsilon_{p_{3/2}}$ and $\epsilon_{p_{1/2}}$. For nuclei in this region, $(p, 2p)$ and $(e, e'p)$ reactions suggest⁵⁰

$$\epsilon_{p_{1/2}} \approx 11 \text{ MeV and } \epsilon_{p_{3/2}} \approx 15.5 \text{ MeV.}$$

However, in ^{27}Al the proton promoted from the $1p$ -shell is strongly attracted by the configuration

that has a single hole in the $d_{5/2}$ shell, and the energies $\epsilon_{p_{1/2}}$ and $\epsilon_{p_{3/2}}$ are greatly reduced.⁵¹ In our first calculation of these states, the 4.055 MeV excitation energy of the first $\frac{1}{2}^-$ level was fitted, at the same time retaining the 4.5 MeV indicated as appropriate for the $1p$ -shell spin-orbit splitting. This calculation left the $\frac{3}{2}^-$ state 0.5 MeV above its observed excitation, but more seriously, underestimated the C3 excitation strength leading to the state by a factor of 12.

In order to generate the missing strength in this transition it was found necessary to introduce appreciable $1p_{3/2}^{-1}$ admixtures into the wave function of the first $\frac{3}{2}^-$ state. The observed excitation energies of the 4.055 and 5.156 MeV levels can be fitted exactly with

$$\epsilon_{p_{1/2}} = 4.01 \text{ MeV and } \epsilon_{p_{3/2}} = 5.35 \text{ MeV,}$$

values corresponding to a $1p$ -shell spin-orbit splitting of only 1.35 MeV. Nevertheless, using these values we obtain the results listed in Tables II and III. It is somewhat remarkable to note that not only is excellent agreement obtained for both the excitation energies and the $B(\text{C}3\uparrow)$ values of the $\frac{1}{2}^-$, 4.055 MeV and $\frac{3}{2}^-$, 5.156 MeV levels, but the calculation also provides a good prediction of the excitation energy and weak transition strength to the probable second $\frac{3}{2}^-$ state at 5.827 MeV.

In an attempt to improve the overall level of agreement between the weak-coupling predictions and the experimental observations, we investigated the effect of assigning to the proton hole an effective charge of $1.5 e$. The improvement was only marginal. At the same time, we have refrained from extending the core-hole interaction [Eq. (13)] to higher order than quadrupole in the belief that, if the weak-coupling interpretation is to be credible, it should be able to reasonably reproduce the observed properties without the introduction of multiple free parameters. Furthermore, the introduction by Singhal⁹ of terms to fourth order yields little improvement in the $B(\text{C}2)$ values calculated for low-lying even-parity states.

VII. CONCLUDING DISCUSSION

The simple strong- and weak-coupling models are seen to provide only partial explanations for the data presented on the odd-parity spectrum of ^{27}Al . In the 6–8 MeV excitation range, the strong-coupling model can account for the C3 excitation strengths to the lowest $\frac{1}{2}^-$, $\frac{3}{2}^-$, $\frac{5}{2}^-$, and $\frac{7}{2}^-$ states, but only at the cost of approximately doubling the Nilsson coefficient G_{E3} . Furthermore, not only is the strength of the $\frac{9}{2}^-$, 7.228 MeV poorly given, but the model also fails to account for the probable

existence of a second $\frac{7}{2}^-$ state at 7.477 MeV. In part, these problems may reflect the existence of band mixing, which is readily apparent in the properties observed for the $1p$ -hole states at 4.055 and 5.156 MeV. Moreover, as pointed out by Bhatt⁵ and others,⁵² the single-particle Nilsson model is fundamentally incapable of explaining the rich detail of the ^{27}Al inelastic spectrum; the energy required to recouple a pair of $d_{5/2}$ nucleons may be less than that required to promote the unpaired nucleon. Such coupling effects have been noted in the even-parity spectrum.⁵³ In this regard, it would therefore be worthwhile to have available a calculation which represented ^{27}Al as three sd -shell particles moving in Nilsson orbitals about a deformed $A = 24$ core.

It has been shown that the weak-coupling model can provide a reasonable description of the odd-parity level scheme. However, although C3 excitation strengths to states in the 6–8 MeV excitation region are less satisfactorily given, perhaps the greatest difficulty is encountered in the interpretation of the lowest-lying even-parity states.

In large part, these problems are attributable to fundamental defects which become apparent in the weak-coupling model when it is examined from a microscopic viewpoint. Some of these weaknesses lie in the nature of the $1d_{5/2}$ hole states, in which the hole is coupled into a subshell that is already actively depopulated in the formation of the excited ^{28}Si core states.⁵⁴ For example, the core states undoubtedly contain strong components with two holes in the $d_{5/2}$ shell.¹ When another $d_{5/2}$ hole is coupled to such a configuration the pairing energy will make it much easier for a nucleon promoted into the $2s_{1/2}$ or $1d_{3/2}$ subshells to drop back to the $d_{5/2}$ shell. To some extent, such components could be included in the calculation by coupling $2s_{1/2}$ and $1d_{3/2}$ holes to the ^{28}Si core states, however, care must be taken to ensure that the orthogonality of the basis states is not jeopardized.⁵⁴

This objection is less easily applied to the case of the $1p$ -hole states, so perhaps it is not surprising that this is where the weak-coupling model seems to enjoy its greatest success. However, in order to account for the excitation energy and observed transition strength of the $\frac{3}{2}^-$, 5.156 MeV state, it is necessary that the $1p$ -shell spin-orbit splitting be set equal to 1.35 MeV, in contrast to the 4.5 MeV indicated by experimental measurements,⁵⁰ and the 4.25 MeV used by Benson and Flowers⁴⁶ in their calculation of low-lying odd-parity states in the ^{19}F spectrum. The reasons for this discrepancy are unclear.

ACKNOWLEDGMENTS

We are indebted to the many people who assisted

in the data taking during the long course of this experiment: Dr. K. Itoh, Dr. F. J. Kline, Dr. S. Kowalski, Dr. R. A. Lindgren, Dr. G. A. Peterson, Dr. D. V. Webb, Dr. C. F. Williamson, and Dr. R. C. York. Helpful communications from Dr. L. W. Fagg and Dr. R. P. Singhal are gratefully acknowledged. The continued encouragement given

throughout this project by Professor G. A. Peterson and our other colleagues at the University of Massachusetts is deeply appreciated. Special thanks are due to Lyman Stinson. This work was financially supported by the U. S. Department of Energy.

- *Present address: School of Physics, Shizuoka University, Shizuoka 422, Japan.
- † Present address: Bates Linear Accelerator, P.O. Box 95, Middleton, Mass. 01949.
- ‡ Present address: I.K.O., Postbus 4395, Amsterdam 1006, Netherlands.
- ¹B. H. Wildenthal and J. B. McGrory, *Phys. Rev. C* **7**, 714 (1973).
- ²B. J. Cole, A. Watt, and R. R. Whitehead, *J. Phys. G* **1**, 935 (1975).
- ³M. J. A. de Voigt, P. W. M. Glaudemans, J. de Boer, and B. H. Wildenthal, *Nucl. Phys.* **A186**, 365 (1972).
- ⁴P. M. Endt and C. van der Leun, *Nucl. Phys.* **A310**, 1 (1978).
- ⁵K. H. Bhatt, *Nucl. Phys.* **39**, 375 (1962).
- ⁶C. L. Lin and F. J. Kline, *Proceedings of the Sendai Conference on Electro- and Photoexcitations. Supp. to Research Report of Lab. of Nucl. Sci., Tohoku University* **10**, 181 (1977).
- ⁷H. Röpke, V. Glattes, and G. Hammel, *Nucl. Phys.* **A156**, 477 (1970).
- ⁸H. G. Price, P. J. Twin, A. N. James, and J. F. Sharpey-Schafer, *J. Phys. A* **7**, 1151 (1974).
- ⁹R. P. Singhal, A. Johnston, W. A. Gillespie, and E. W. Lees, *Nucl. Phys.* **A279**, 29 (1977).
- ¹⁰V. K. Thankappan, *Phys. Rev.* **141**, 957 (1966).
- ¹¹D. Evers, J. Hertel, T. W. Retz-Schmidt, S. J. Skorka, *Nucl. Phys.* **A91**, 472 (1967).
- ¹²R. M. Lombard and G. R. Bishop, *Nucl. Phys.* **A101**, 625 (1967).
- ¹³G. M. Crawley and G. T. Garvey, *Phys. Lett.* **19**, 228 (1965).
- ¹⁴J. W. Maas, A. J. C. D. Holvast, A. Baghus, H. J. M. Aarts, and P. M. Endt, *Nucl. Phys.* **A301**, 237 (1978).
- ¹⁵H. Röpke, V. Glattes, and G. Hammel, *Nucl. Phys.* **A172**, 506 (1971).
- ¹⁶S. G. Nilsson, *K. Dan. Vidensk. Selsk. Mat. Fys. Medd.* **29**, No. 16 (1955).
- ¹⁷R. M. Lombard and G. R. Bishop, *Nucl. Phys.* **A101**, 601 (1967).
- ¹⁸T. Terasawa, K. Nakahara, M. Oyamada, H. Saito, and E. Tanaka, *Kakauriken Kenkyu Hokoku* **4**, 27 (1972).
- ¹⁹P. C. Dunn, *Nucl. Instrum.* **165**, 163 (1979).
- ²⁰S. Kowalski, W. Bertozzi, and C. P. Sargent, in 1967 MIT Summer Study: Medium Energy Nuclear Physics with Electron Linear Accelerators. L.N.S. Report TID-24667, USAEC, 1967 (unpublished), p. 39.
- ²¹J. Haimson, *IEEE Trans. Nucl. Sci.* **20**, 914 (1973).
- ²²W. Bertozzi, M. V. Hynes, C. P. Sargent, W. Turchinetz, and C. F. Williamson, *Nucl. Instrum.* **162**, 211 (1979).
- ²³W. Bertozzi, M. V. Hynes, C. P. Sargent, C. Creswell, P. C. Dunn, A. Hirsch, M. Leitch, B. E. Norum, F. N. Rad, and T. Sasanuma, *Nucl. Instrum.* **141**, 457 (1977).
- ²⁴R. S. Hicks, private communication.
- ²⁵G. A. Peterson, J. B. Flanz, D. V. Webb, H. deVries, and C. F. Williamson, *Nucl. Instrum. Methods* **160**, 375 (1979).
- ²⁶H. Überall, *Electron Scattering from Complex Nuclei* (Academic, New York, London, 1971).
- ²⁷H. Crannell, internal report, Catholic University, Washington D.C. (1977).
- ²⁸J. C. Bergstrom, in 1967 MIT Summer Study: Medium Energy Nuclear Physics with Electron Linear Accelerators, L.N.S. Report No. TID-24667, USAEC, 1967 (unpublished), p. 251.
- ²⁹I. P. Auer and J. C. Bergstrom, FORTRAN program IPA, unpublished notes (1975).
- ³⁰I. Sick and J. S. McCarthy, *Nucl. Phys.* **A150**, 631 (1970).
- ³¹F. Borkowski, P. Peuser, G. G. Simon, V. H. Walther, and R. D. Wendling, *Nucl. Phys.* **A222**, 269 (1974).
- ³²T de Forest and J. Walecka, *Adv. Phys.* **15**, 1 (1966).
- ³³D. G. Ravenhall and D. R. Yennie, *Proc. Phys. Soc. London* **A70**, 857 (1957).
- ³⁴R. S. Hicks and A. Hotta, private communication.
- ³⁵T. Stovall, D. Vinciguerra, and M. Bernheim, *Nucl. Phys.* **A91**, 513 (1967).
- ³⁶C. W. deJager, H. deVries, and C. deVries, *At. Data Nucl. Data Tables* **14**, 479 (1974).
- ³⁷A. E. Litherland, H. McManus, E. B. Paul, D. A. Bromley, and H. E. Gove, *Can. J. Phys.* **36**, 378 (1958).
- ³⁸A. A. Pilt, *Z. Naturforsch* **32A**, 73 (1977).
- ³⁹D. A. Bromley, H. E. Gove, and A. E. Litherland, *Can. J. Phys.* **35**, 1057 (1957).
- ⁴⁰A. Christy and O. Häusser, *Nucl. Data Tables* **11**, 281 (1972).
- ⁴¹G. Mulhaupt, Ph.D. thesis, Universität Mainz, 1970 (unpublished).
- ⁴²K. Whitner and C. F. Williamson, private communication (1979).
- ⁴³S. W. Brain, A. Johnston, W. A. Gillespie, E. W. Lees, and R. P. Singhal, *J. Phys. G* **3**, 681 (1977).
- ⁴⁴V. K. Thankappan and W. W. True, *Phys. Rev.* **137**, B793 (1965).
- ⁴⁵A. Johnston, Internal Report, Kelvin Laboratory, University of Glasgow (1975).
- ⁴⁶H. G. Benson and B. H. Flowers, *Nucl. Phys.* **A126**, 305 (1969).
- ⁴⁷B. H. Wildenthal and E. Newman, *Phys. Rev.* **167**, 1027 (1968).

- ⁴⁸H. Mackh, G. Mairle and G. J. Wagner, *Z. Phys.* 269, 353 (1974).
- ⁴⁹J. D. MacArthur, *Bull. Am. Phys. Soc.* 17, 90 (1972).
- ⁵⁰R. C. Barrett and D. F. Jackson, *Nuclear Sizes and Structure* (Clarendon, Oxford, 1977), p. 370.
- ⁵¹G. J. Wagner, *Phys. Lett.* 26B, 429 (1968).
- ⁵²D. M. Brink and A. K. Kerman, *Nucl. Phys.* 12, 314 (1959).
- ⁵³H. Röpke, P. Betz, G. Bender, V. Glattes, G. Hammel, and W. Brendler, *Z. Phys.* 268, 391 (1974).
- ⁵⁴M. H. Macfarlane and J. B. French, *Rev. Mod. Phys.* 32, 567 (1960).